Enhanced method for the generation of binary Fresnel holograms based on grid-cross downsampling

W. K. Cheung[1*], Peter Tsang[1], T. C. Poon[2,3], and Changhe Zhou (周常河)[3]

[1]*Department of Electronic Engineering, City University of Hong Kong, Tat Chee Avenue, Kowloon, Hong Kong, China*

[2]*Bradley Department of Electrical and Computer Engineering, Virginia Tech, USA*

[3]*Shanghai Institute of Optics and Fine Mechanics, Chinese Academy of Sciences, Shanghai 201800, China*

[*]*Corresponding author: 50695250@student.cityu.edu.hk*

Received July 30, 2011; accepted September 9, 2011; posted online November 18, 2011

Past research has demonstrated that digital Fresnel holograms can be binarized in a non-iterative manner by downsampling the source image with a grid lattice prior to the hologram generation process. The reconstructed image of a hologram that is binarized with this approach is superior in quality compared with that obtained with direct thresholding, half-toning, and error diffusion. Despite the success, the downsampling mechanism results in a prominent texture of regularly spaced voids in the shaded regions. To alleviate this problem, an enhanced non-iterative method for the generation of binary Fresnel holograms is presented. Our method is based on a multi-direction line-sampling formed by a combined grid and cross lattice, which is capable of preserving a more solid texture in the shaded regions and enhancing the visual quality of the reconstructed image. Computer simulations and optical reconstructions are shown to demonstrate the effectiveness of our proposed technique.

OCIS codes: 090.0090, 090.1760, 090.1995.

doi: 10.3788/COL201109.120005.

The rapid advancement of computing technology in the past decade has enabled holograms of three-dimensional (3D) objects to be constructed with numerical means. Such approach, commonly known as computer-generated holography (CGH)[1,2], has been identified as an important area in digital holography (DH). Among other problems, one of the major concerns in the research of DH is the realization of holograms for optical reconstruction. Holograms are desired to be produced with affordable printing devices, from both the academic and commercial perspectives. Evidently, such approach is more economical and faster than the hardcopying of holograms with expensive fringe writers[3]. However, although the resolutions of some contemporary laser printers[4] are sufficiently high for printing fringe patterns in the order of microns, the majority are only capable of outputting black and white dots. This means that holograms have to be binarized prior to printing. Apart from the printing issue, the binary hologram has the advantage of having lesser data size than a gray hologram. On the downside, the binarization of hologram leads to the degradation of the reconstructed image. Attempts have been made in the past to address the distortions caused by the quantization of holograms. Although some of them may not be directly related to hologram binarization, they nevertheless provide some insights into the problem. These include the work reported in Refs. [5–11]. Methods on the generation of binary holograms in an iterative manner have been reported in Refs. [12–14]. However, to our knowledge, little work has been done on the analysis and generation of binarized Fresnel CGHs in a non-iterative manner. A straightforward approach is sign thresholding, in which hologram pixels with positive and negative values are binarized to white and black intensities, respectively. A hologram binarized in this manner is incapable of preserving the shaded regions (i.e., areas with smooth or homogeneous intensity variation), and only the edges are present in the reconstructed images. Moderate success has been attained in applying error diffusion[15] in the binarization of Fourier[16−18] and Fresnel[19] holograms. However, the reconstructed images are contaminated with noise. An alternative method has been reported in Ref. [20] with the integration of grid line downsampling and sign thresholding, which provides a better preservation of the shaded regions in the reconstructed image and with less amount of noise contamination. Despite the success, the shaded regions are filled with a texture of uniformly spaced holes that are rather prominent in the reconstructed image. In this letter, a solution on multi-direction line-sampling is proposed to alleviate this problem. The principles of CGH are briefly outlined. The distortion caused by the binarization of the hologram through sign thresholding is also illustrated. We then describe the pros and cons of the method in Ref. [20], which is developed to reduce the artifacts caused by sign thresholding. Our proposed scheme and its evaluation are presented. This is then followed by a conclusion summarizing the essential findings of this study.

We first explain the distortion caused by binarization via sign thresholding. The improved method in Ref. [20], which is applied to rectify the problem, is then outlined. We consider an on-axis Fresnel hologram $H(x, y)$ that is generated from a 3D surface. Each point on the surface is assumed to be self-illuminating, and its intensity $I(u, v)$ is shown in Fig. 1. The distance of a point at position (u, v) to the hologram along the z direction is denoted by $w_{u,v}$.

The hologram can be derived from the summation of the contribution of individual object points, each casting a Fresnel zone plate on $H(x, y)$, given as[21]

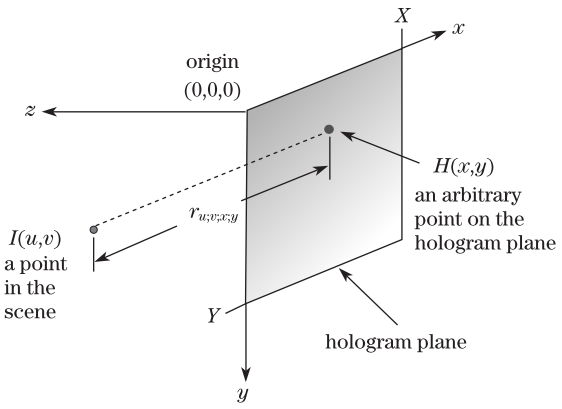

Fig. 1. Spatial relation between an object point and a hologram point.

$$H(x,y)\Big|_{\substack{0\leqslant x<X\\0\leqslant y<Y}} = \sum_{u=0}^{X-1}\sum_{v=0}^{Y-1}\frac{I(u,v)\exp(\mathrm{i}2\pi r_{u;v;x;y}/\lambda)}{r_{u;v;x;y}}, \quad (1)$$

where $I(u,v)$ and $r_{u;v;x;y}=\sqrt{(x-u)^2+(y-v)^2+w_{u;v}^2}$ are the intensity of the point located at (u,v) in the 3D scene and its distance to the hologram, respectively. Here, λ is the wavelength of the optical beam. X and Y are the horizontal and vertical extents of the hologram, respectively; without the loss of generality, they are assumed to be identical to that of the image scene.

In a straightforward manner, the real and the imaginary parts of the hologram can be binarized with sign thresholding, in which the positive and negative pixel values are truncated to white and black intensities, respectively. However, as shown in Ref. [20], the hologram binarized with this approach results in a significant removal of the shaded or homogeneous region(s), and an emphasis of the edges, in the reconstructed image.

To overcome this problem, the intensity image $I(x,y)$ is downsampled by a square grid lattice prior to its conversion to a hologram, as proposed in Ref. [20]. Mathematically, $I(x,y)$ is downsampled to a new image $I_{\mathrm{D}}(x,y)$ given as

$$I_{\mathrm{D}}(x,y)=I_1(x,y)\cup I_2(x,y), \quad (2)$$

$$I_1(x,y)=\begin{cases}I(x,y) & x=\tau M\\ 0 & \text{otherwise}\end{cases},$$

$$I_2(x,y)=\begin{cases}I(x,y) & y=\tau M\\ 0 & \text{otherwise}\end{cases},$$

where τ is an integer running from $0,\pm1,\pm2,\cdots$, and M is the downsampling factor that determines the spacing between adjacent grid lines. The operator $\cup$ denotes the union of two sets of data, namely $I_1(x,y)$ and $I_2(x,y)$, and represents the downsampling of with a uniform grid of vertical and horizontal lines, respectively. The Fourier transforms of the line samples $I_1(x,y)$ and $I_2(x,y)$, which are denoted by $\tilde{I}_1(\omega_x,\omega_y)$ and $\tilde{I}_2(\omega_x,\omega_y)$, respectively, are given as

$$\tilde{I}_1(\omega_x,\omega_y)=\frac{1}{M}\sum_{n=-(M-1)}^{M-1}\tilde{I}\Big(\omega_x,\omega_y-\frac{2\pi n}{M}\Big), \quad (3)$$

$$\tilde{I}_2(\omega_x,\omega_y)=\frac{1}{M}\sum_{n=-(M-1)}^{M-1}\tilde{I}\Big(\omega_x-\frac{2\pi n}{M},\omega_y\Big), \quad (4)$$

where ω_x and ω_y are the spatial frequencies associated with coordinates x and y, respectively.

Assuming that the bandwidth of the source image is limited to avoid the aliasing error (i.e., the bandwidth of $I(x,y)$ is less than π/M rad/s), the outcome of the grid sampling, according to Eqs. (3) and (4), is given as

$$\tilde{I}_{\mathrm{D}}(\omega_x,\omega_y)=\tilde{I}_1(\omega_x,\omega_y)\cup\tilde{I}_2(\omega_x,\omega_y). \quad (5)$$

The frequency spectrum is illustrated in Fig. 2. The downsampling by the vertical and horizontal sets of grid lines produces multiple replica images of the baseband spectrum along the horizontal and vertical frequency axes. Each replica image is separated from its immediate neighbor by $2\pi/M$ rads/s, which tends to extend the high-frequency contents of the source image and hologram before binarization. Experimental results reveal that grid downsampling is effective in patching the empty space in the shaded or homogeneous regions, which are removed when the hologram is binarized with sign thresholding.

However, the patching content is in the form of a grid texture that appears as a uniform array of square holes. This weakens the overall intensity and degrades the visual quality of the reconstructed image.

The shortcoming in Ref. [20], can be easily explained by the replacement of the original image $I(x,y)$ by its downsampled version $I_{\mathrm{D}}(x,y)$ in the generation of the hologram. Hence, although the frequency extension mechanism along the horizontal and vertical directions is effective in preserving a reasonable reconstructed image of $I_{\mathrm{D}}(x,y)$ after the hologram is binarized, the missing

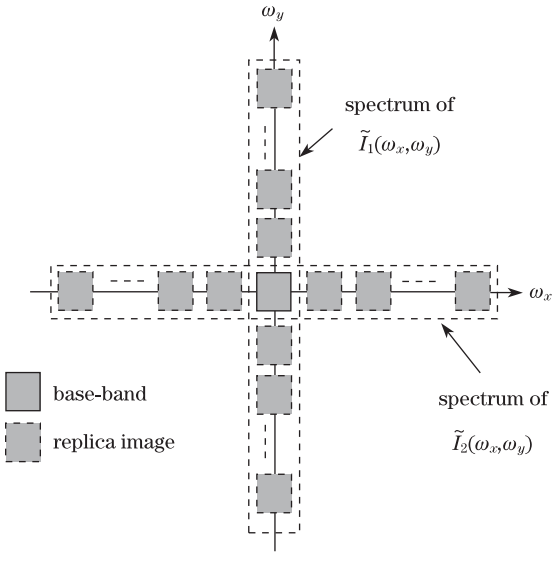

Fig. 2. Frequency spectrum of $I_{\mathrm{D}}(x,y)$.

information in between the grid lattice is lost. Intuitively, this can be overcome by adding more sampling points to increase the density of $I_{\mathrm{D}}(x,y)$. However, simply increasing the sample points could modify the frequency spectrum, such that the replica images interfere with each other in a destructive manner. As a result, the high-frequency components are weakened and the quality of the reconstructed image is degraded. The above dilemma suggests that the sampling points must be increased in such a way that it will not affect the frequency extension mechanism. In view of this, we propose the multi-directional line-sampling method that is described as follows. Referring to Eqs. (3) and (4), as well as to Fig. 2, the grid downsampling lattice described in Ref. [20] shows that the direction along which the replicas of the baseband spectrum are generated in the frequency space and the direction of downsampling along the spatial domain are all identical. For example, $I_1(x,y)$, which is derived from downsampling $I(x,y)$ along the y axis with a regular sequence of vertical lines, constitutes to a strip of uniformly spaced replica images of the baseband spectrum along the horizontal frequency axis ω_y. Similar association can be made between $I_2(x,y)$ and the sequence of replica images along the vertical frequency axis ω_x. This indicates that the sparsity of the spatial domain (which resulted from downsampling) and the frequency space are directly related. On this basis, we propose to add to the frequency spectrum of $I_{\mathrm{D}}(x,y)$ a sequence of repeated, non-overlapping replica images of the baseband spectrum along the $\pm 45^\circ$ directions, as shown in Fig. 3. The rationale of adopting such mechanism is given as follows. Firstly, the newly added frequency bands increased the compactness of the spectrum, hence the density of the spatial image. Secondly, similar to the downsampling with a grid lattice, the series of replica images along the two diagonal axes extended the high-frequency contents, hence enabling them (and the associated fringe patterns) to survive after the binarization process. Thirdly, the newly added frequency bands are non-overlapping with the original ones shown in Fig. 2. If the pair of diagonal frequency spectra are added at other angles instead of $\pm 45^\circ$, they may overlap with $\tilde{I}_1(\omega_x,\omega_y)$ and $\tilde{I}_2(\omega_x,\omega_y)$.

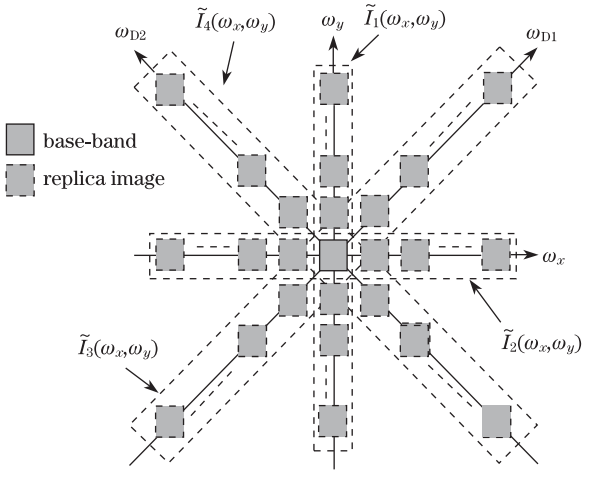

Fig. 3. Proposed frequency spectrum of the downsampled source image for increasing the density of the reconstructed image.

Fourthly, as will be explained below, the introduction of the diagonal spectra can be easily realized by downsampling the original image along the $\pm 45^\circ$ directions. The above mentioned factors imply that the pair of additional strips of frequency spectra will increase the density of the reconstructed image along the diagonal directions, without affecting the contributions of the object points that are sampled by the square grid. Mathematically, the revised frequency spectrum in Fig. 3 can be expressed as

$$\tilde{I}'_{\mathrm{D}}(\omega_x,\omega_y) = \tilde{I}_{\mathrm{D}}(\omega_x,\omega_y) \cup \tilde{I}_3(\omega_x,\omega_y) \cup \tilde{I}_4(\omega_x,\omega_y), \quad (6)$$

where $\tilde{I}_3(\omega_x,\omega_y)$ and $\tilde{I}_4(\omega_x,\omega_y)$ denote the sequences of replica images of the baseband spectrum along the $\pm 45^\circ$ directions.

We then derive the downsampling image $I'_{\mathrm{D}}(x,y)$ in the spatial domain, which results in the frequency spectrum $\tilde{I}'_{\mathrm{D}}(\omega_x,\omega_y)$ in Eq. (6). As the replica images are non-overlapping, the line samples $I_1(x,y)$ and $I_2(x,y)$ corresponding to the first term $\tilde{I}_{\mathrm{D}}(\omega_x,\omega_y)$ of the equation are retained in the downsampled image $I'_{\mathrm{D}}(x,y)$. The additional frequency bands, namely $\tilde{I}_3(\omega_x,\omega_y)$ and $\tilde{I}_4(\omega_x,\omega_y)$, correspond to a pair of downsampling images given as

$$I_3(x,y) = \begin{cases} I(x,y) & (x \bmod M) = (y \bmod M) \\ 0 & \text{otherwise} \end{cases}, \quad (7)$$

$$I_4(x,y) = \begin{cases} I(x,y) & (x \bmod M) = [(M-1) - (y \bmod M)] \\ 0 & \text{otherwise} \end{cases}, \quad (8)$$

where mod is the modulo operator and $I_3(x,y)$ and $I_4(x,y)$ are the inverse Fourier transforms of $\tilde{I}_3(\omega_x,\omega_y)$ and $\tilde{I}_4(\omega_x,\omega_y)$, respectively. We note that Eqs. (7) and (8) represent the downsampling of the source image $I(x,y)$ by a pair of regularly spaced diagonal line sequences that are orthogonal to each other and take the form of a cross pattern. As an example, the sampling lattice of our proposed method between the interval $(0 \leqslant x \leqslant M)$ and $(0 \leqslant y \leqslant M)$ for $M = 8$ is shown in Fig. 4, where the dot symbol "•" represents the sample point where the pixels in $I(x,y)$ are preserved in $I'_{\mathrm{D}}(x,y)$. For the rest of the area in the downsampled image, the pixels are removed and set to zero value.

The planar image shown in Fig. 5(a), which is parallel to the hologram and largely comprising shaded areas, is employed as a test sample to demonstrate the performance of our proposed method. The source image is positioned at a distance of 0.4 m from the hologram. Based on the optical setting in Table 1, Eq. (1) is applied to generate two on-axis holograms: one with the source image downsampled with a factor of 16 on a square grid lattice (Fig. 5(b)) and the other with the proposed grid-cross lattice (Fig. 5(c)). The source image has been low-pass filtered to prevent the aliasing error.

The on-axis complex holograms are each converted into a real off-axis hologram $H_{\mathrm{OF}}(x,y)$ by adding a planar reference beam $R(y)$, which is inclined at an angle of 1.2° along the vertical direction. The off-axis hologram is then given by $H_{\mathrm{OF}}(x,y) = \mathrm{Re}[H(x,y) \cdot R(y)]$, where

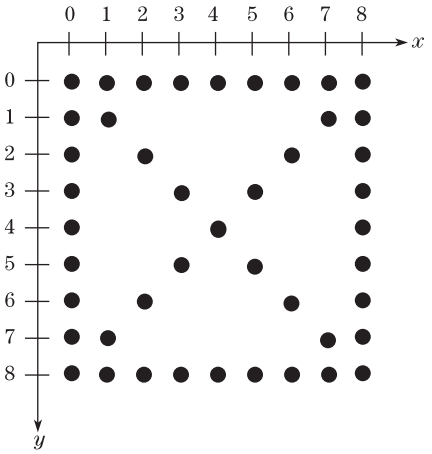

Fig. 4. Sampling lattice of our proposed method.

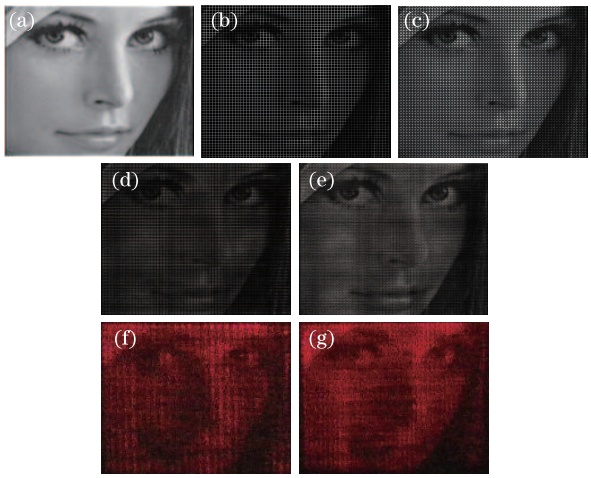

Fig. 5. (a) Test planar image positioned at a distance of 0.4 m from the hologram; downsampling of the image in (a) with (b) grid line sampling lattice and (c) multi-directional line sampling (grid-cross) lattice; simulation for the reconstructed image of the hologram representing the image (a) binarized with (d) line-sampling method[20] and (e) proposed grid-cross sampling method; optical reconstructed image of the hologram representing the image in (a) binarized with (f) line-sampling method[20] and (g) proposed grid-cross sampling method.

Table 1. Optical Setting Adopted in the Hologram Generation Process

Object Size (pixel)	640 × 640
Hologram Size (pixel)	1 024 × 1 024 (about 1 × 1 (cm))
Pixel Size of the Hologram (μm^2)	10.583
Wavelength of Light (nm)	650

Re $[\cdot]$ stands for taking the real part of the quantity being bracketed.

Subsequently, we convert the holograms into bi-level representations based on the sign binarization. The numerical reconstructed images are shown in Figs. 5(d) and (e). The images that are downsampled with the grid-cross lattice are brighter and contain more details than those downsampled by the grid lattice. The binarized holograms are then produced with a printer with 2 400 dpi on Agfa red-sensitive films and are illuminated by a laser beam for optical reconstruction. The optical reconstructed images are shown in Figs. 5(f) and (g). The reconstructed image corresponding to the binarized hologram prepared by the method in Ref. [20] (i.e., utilizing a grid lattice) is weaker in intensity and exhibits a prominent grid pattern. However, the reconstructed image of the hologram generated by our proposed method (i.e., utilizing a grid-cross lattice) is brighter and can preserve the finer details of the source image. The results are in line with the ones obtained with numerical reconstruction.

Similar treatment is applied to the sample image shown in Fig. 6(a), which is evenly divided into a top section (containing a star symbol) and a bottom section (containing a heart symbol) positioned at 0.3 and 0.4 m from the hologram, respectively. Both symbols are filled with solid white intensity. The binary holograms are generated and printed with the same procedure as in the previous test sample. The optical reconstructed images obtained by illuminating the binarized holograms with a laser beam are shown in Figs. 6(b)–(e). Our proposed grid-cross sampling method results in better reconstructed images at both depth planes.

Finally, we illustrate the effect of the downsampling factor M on our proposed method. Grid-cross downsampling is applied to the image in Fig. 5(a) with $M = 12$, 16, and 24. The numerical reconstructed images of the holograms generated from the three downsampled images are shown in Figs. 7(a)–(c). For the smaller value of $M = 12$, the shaded area is poorly reconstructed. When M increases, the shaded area is better preserved; however, the resolution is degraded accordingly. A good compromise between these two conflicting factors is met with a moderate value of $M = 16$.

In conclusion, binary Fresnel hologram can be generated by first downsampling the source image with a horizontal and a vertical sequence of evenly spaced straight lines that combine to form a square grid lattice. Subsequently, the downsampled image is converted into a Fresnel hologram and then converted to a bi-level representation via sign binarization. The reconstructed images of the binary holograms generated with this approach are capable of preserving, to a certain extent, the shaded and homogeneous regions. However, the downsampling

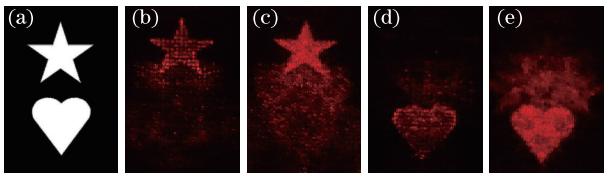

Fig. 6. (a) Test image comprising an upper section and a lower section, positioned at a distance of 0.3 and 0.4 m from the hologram, respectively; optical reconstructed image at a distance of 0.3 m of the hologram representing the image in (a), binarized with (b) line-sampling method[20] and (c) proposed grid-cross sampling method; optical reconstructed image at a distance of 0.4 m of the hologram representing the image in (a) binarized with (d) line-sampling method[20] and (e) grid-cross sampling proposed.

Fig. 7. Simulation for the reconstructed image of the hologram representing the image in Fig. 5(a) binarized with the proposed grid-cross sampling method with (a) $M = 12$, (b) $M = 16$, and (c) $M = 20$.

mechanism also leads to a grid texture of empty holes, which weakens the brightness and removes a considerable amount of detailed information in the void areas. In this letter, we propose a new method of downsampling the source image so that the blank areas can be reduced in the reconstructed image. We analyze the frequency spectrum of the downsampled source image and find that the sparsity of the spatial domain and the frequency space are directly related. Although the density of the spatial image can be increased by simply adding more sample points, the replica images in the frequency spectrum, which are mandatory in preserving the shaded regions in the reconstructed image, may interfere in a destructive manner. In view of this problem, we propose to superimpose, on top of the original square grid lattice, a cross-line lattice. The latter is derived by simply adding an original square grid lattice rotated by 45° along the counterclockwise direction. The proposed sampling lattice (grid-cross lattice) leads to additional non-overlapping replica images, thereby decreasing the sparsity of the frequency spectrum without causing interference among the replica images. The numerical and optical reconstructions of the binary holograms reveal that the reconstructed images of binary holograms prepared by our proposed method are superior in quality than those obtained based on the existing method reported in Ref. [20]. More specifically, our method results in reconstructed images that are brighter, visually pleasing, and have the capability to preserve finer details on the source images.

This work was partly supported by the Chinese Academy of Sciences Visiting Professorship for Senior International Scientists Program Under Grant No. 2010T2G17.

References

1. A. W. Lohmann and D. P. Paris, Appl. Opt. **6,** 1739 (1967).
2. B. R. Brown and A. W. Lohmann, IBM J. Res. Dev. **13,** 160 (1969).
3. H. Yoshikawa and M. Tachinami, Proc. SPIE **5742,** 259 (2005).
4. L. C. Ferri, Computers & Graphics **25,** 309 (2001).
5. V. V. Krishna and P. S. Naidu, Proc. SPIE **813,** 397 (1987).
6. E. Zhang, S. Noehte, C. H. Dietrich, and R. Manner, Appl. Opt. **34,** 5987 (1995).
7. B. Zhao and Y. Surrel, Appl. Opt. **36,** 2070 (1997).
8. G. A. Mills and I. Yamaguchi, Appl. Opt. **44,** 1216 (2005).
9. A. J. Cable, E. Buckley, P. Marsh, N. A. Lawrence, T. D. Wilkinson, and W. A. Crossland, SID 04 Digest, 1431 (2004).
10. S. Nozaki and Y. Chen, in *Proceedings of Fifth International Conference on Natural Computation* 13 (2009).
11. I. Moreno, A. Martínez-García, L. Nieradko, C. Gorecki, and J. Albero, J. Europ. Opt. Soc. **5,** 10011 (2010).
12. M. P. Chang and O. K. Ersoy, Appl. Opt. **32,** 3122 (1993).
13. E. Zhang, S. Noehte, C. H. Dietrich, and R. Männer, Appl. Opt. **34,** 5987 (1995).
14. B. B. Chhetri, S. Yang, and T. Shimomura, Opt. Eng. **40,** 2718 (2001).
15. R. W. Floyd and L. Steinberg, Proc. Soc. Inf. Display **17,** 75 (1976).
16. R. Eschbach, Appl. Opt. **30,** 3702 (1991).
17. R. Eschbach and Z. Fan, Appl. Opt. **32,** 3130 (1993).
18. R. L. Easton, R. Eschbach, and R. Nagarajan, J. Modern Opt. **43,** 1219 (1996).
19. F. Fetthauer, S. Weissbach, and O. Bryngdahl, Opt. Commun. **114,** 230, (1995).
20. P. Tsang, T. Poon, W. Cheung, and J. Liu, Appl. Opt. **50,** B88 (2011).
21. T. Poon, *Digital Holography & Three-Dimensional Display: Principles & Applications* (Springer, New York, 2006).